Bulk AlN crystal growth by direct heating of the source using microwaves

D. Zhuang[a], J.H. Edgar[a,*], B. Liu[a], H.E. Huey[b], H.X. Jiang[c], J.Y. Lin[c], M. Kuball[d], F. Mogal[e], J. Chaudhuri[e], Z. Rek[f]

[a] *Department of Chemical Engineering, Kansas State University, Manhattan, KS 66506-5102, USA*
[b] *Micramics, Inc., 945 Berryessa Rd. #5, San Jose, CA 95133, USA*
[c] *Department of Physics, Kansas State University, Manhattan, KS 66506, USA*
[d] *H.H. Wills Physics Laboratory, University of Bristol, Bristol BS8 1TL, UK*
[e] *Department of Mechanical Engineering, Wichita State University, Wichita, KS 67260, USA*
[f] *Stanford Linear Acelerator Center, 2575 Sand Hill Road, Mail Stop 69, Menlo Park, CA 94025, USA*

Abstract

AlN single crystal platelets up to $2 \times 3\,mm^2$ and needles 1 mm in diameter and 3 mm in length were successfully grown by directly heating the source materials with microwaves. The process temperature was over $2000°C$ and the pressure was kept constant at 910 Torr. The growth rate was typically $300\,\mu m\,h^{-1}$ in the c-direction. An emission around 5.5 eV was observed in the photoluminescence spectrum probably caused by magnesium impurity. The dislocation density was low, $6 \times 10^3\,cm^{-2}$, as determined by both synchrotron white beam X-ray topography and etching in molten potassium hydroxide–sodium hydroxide eutectic alloy. Etching produced hexagonal pits and hexagonal hillocks on the Al- and N-polar surfaces, respectively. Raman spectra, X-ray topograph, and etch pit densities demonstrate that the crystals have good structural quality.
© 2003 Elsevier B.V. All rights reserved.

PACS: 61.72; 78.30; 78.55; 81.10

Keywords: A1. Characterization; A1. Etching; A1. X-ray topography; A2. Single crystal growth; B1. Nitrides

1. Introduction

Significant progress has been made with group III-nitride semiconductor devices in the past decade. Blue and green LEDs and blue laser diodes fabricated using heteroepitaxial III-nitride films are commercially available, and electronic devices, such as power transistors, have been successfully demonstrated [1,2]. However, high dislocation densities caused by the lattice constant mismatch between group III-nitrides and 6H–SiC and/or sapphire substrates remains an obstacle to

---

*Corresponding author. Tel.: +1-785-532-4320; fax: +1-785-532-7372.

E-mail address: edgarjh@ksu.edu (J.H. Edgar).

the further development of these devices, both in aspects of device lifetime and performance. Since AlN has a small lattice constant mismatch ($\sim 2.4\%$ in *a*-axis [3]) and an almost identical thermal expansion coefficient with GaN, bulk AlN single crystalline substrates for epitaxial GaN film growth should reduce its defects density immensely, triggering an expeditious increase in group III-nitride device quality. In addition, the high thermal conductivity ($340 \, W \, m^{-1} \, K^{-1}$) of AlN makes it suitable for high power applications, where the heat generated by devices must be efficiently dissipated [4]. AlN is also a perfect material for high power microwave devices and UV detectors, due to its high resistivity (10^7–$10^{13} \, \Omega \, cm$) and very wide energy bandgap (6.2 eV).

Though intensive research efforts have been devoted to AlN single crystal growth via sublimation-recondensation method, first validated by Slack and McNelly in the 1970s [5], no bulk AlN substrates with high crystalline quality have yet been commercialized. According to model calculations [6], the main challenge is that the sublimation technique requires a process temperature of more than $2100\,^\circ C$ in order to obtain a viable fast growth rate ($\geqslant 100 \, \mu m \, h^{-1}$). At such an extreme temperatures, furnace fixtures can react with Al or N_2, sublime or even melt. Keeping furnace fixtures at low temperature should reduce production cost of AlN single crystal growth by allowing the crucibles to last longer.

The temperature of the furnace fixtures can be minimized by directly heating the AlN source using microwaves. The advantages of microwave heating to sinter ceramic materials have been recognized for many years [7]. These include efficient use of energy, rapid and more uniform heating. Microwave heating occurs in the body of the ceramic materials with energy being lost from the surface by radiation, conduction, and convection. The temperature gradient is thus opposite to that of traditional heating methods, in which the surface of a body is heated and the interior is heated by conduction. The mechanism of microwave heating of AlN varies with temperature. At room temperature, the free electron concentration in AlN is very low hence its electrical conductivity

is very low (on the order of $10^{-11} \, \Omega^{-1} \, cm^{-1}$). At room temperature, microwave heating occurs by reorientation of the dipoles in the AlN, which is subsequently randomized as heat. As the temperature and therefore the carrier concentration of the AlN increases [8], the heating mechanism changes to more efficient oscillation of conduction electrons. Heating and sintering of AlN ceramics by microwaves has been demonstrated [9].

Oxygen contamination has a vital role when evaluating AlN crystal quality since a high oxygen concentration decreases the thermal conductivity of AlN [10,11] and can cause crystal defects. Slack and McNelly [5] speculated that the peaks at 2.86 eV in AlN photoluminescence (PL) spectra was due to the combination of oxygen impurities and nitrogen vacancies. Harris et al. [10] reported a continuous shift of an oxygen-related PL peak to a lower energy level (4.0–3.3 eV) as the oxygen concentration increases to a critical concentration of about 0.75 at%. Due to the limitation of material quality, few research groups reported near-band-edge emissions, a characteristic of low impurity level and low defect density, in bulk AlN luminescence studies so far. Kuokstis et al. [12] reported their PL spectra of bulk AlN crystals, showing free excitation emission at 5.94 and 5.95 eV for *A*- and *C*-planes, respectively. One AlN sample grown by Slack and McNelly [5] and Slack et al. [13] had a peak position at 4.03 eV and a measured room temperature thermal conductivity of $275 \, W \, m^{-1} \, K^{-1}$. Nevertheless, some groups have successfully demonstrated near-band-edge emission in heteroepitaxial AlN films. In 1998, Tang et al. [14] first reported cathodoluminescence (CL) spectra with free excitons or excitons bound to shallow donor or acceptor impurities at 6.11 eV, from an undoped AlN sample grown on sapphire substrate. More recently, bandedge emission lines at 5.96 and 6.015 eV have been observed in AlN epilayers by deep UV (down to 196 nm) PL spectroscopy measurement [15,16]. Mg-doped AlN epilayers have also been studied and an activation energy of about 0.51 eV for Mg acceptors in AlN has been determined [17].

In this communication, we present the development of AlN single crystals growth by a microwave-heated furnace employing the

sublimation-recondensation method, and the characterization of these crystals.

2. Experimental procedure

Fig. 1 shows a cross section view of the growth reactor used in this experiment developed by Micramics, Inc. Two separate 3 kW variable power supplies provide the microwaves for the sublimation process. The AlN source is contained in a cylindrical pyrolytic boron nitride (pBN) crucible. This crucible is packed in hexagonal BN powder contained inside a pBN retort. The pBN containers are surrounded by alumina insulation, and the entire arrangement is held in a stainless steel chamber. The alumina insulation is transparent to microwaves, but is thermally insulating ($k = 0.39\,\mathrm{W\,m^{-1}\,K^{-1}}$ at $1650°C$). The BN powder acts as additional insulation and helps to absorb the microwave energy. A computer controlled tuning plate at the bottom of chamber was

adjusted to minimize microwave reflection by moving up and down. The source temperature and crucible sidewall temperature were measured by two color infrared pyrometers from the top and side viewpoint, respectively. The growth time was varied from 12 h to 24 h and the chamber pressure was kept constant at 910 Torr N_2.

Defect levels and crystalline quality were analyzed by PL and Raman spectrum, respectively. In the PL study, the AlN samples were excited at a wavelength of 196 nm. Raman spectra were recorded from the samples using a Renishaw micro-Raman system with the 488 nm line of an Ar^+ ion laser as excitation sources. The synchrotron topography experiments were carried out at the Synchrotron Radiation Topography experimental station 2.2 at the Stanford Synchrotron Radiation Laboratory, Stanford, CA. Transmission topographs were taken using Laue diffraction technique and white beam radiation. The dislocation density was estimated by etching in molten eutectic KOH/NaOH and synchrotron white beam

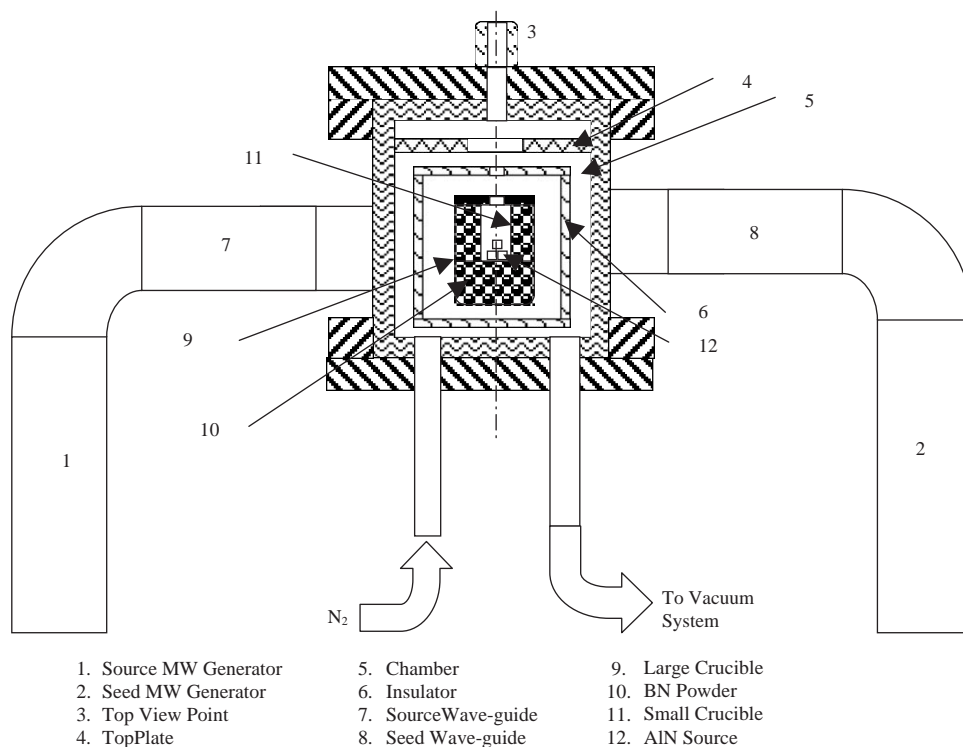|		
1. Source MW Generator	5. Chamber	9. Large Crucible
2. Seed MW Generator	6. Insulator	10. BN Powder
3. Top View Point	7. SourceWave-guide	11. Small Crucible
4. TopPlate	8. Seed Wave-guide	12. AlN Source

Fig. 1. Cross section view of growth reactor.

X-ray topography (SWBXT). A series of eutectic etchings were performed to optimize etching parameters. The final etching parameters for Al-polar crystal were at temperature of 380°C and for 3 min.

3. Results and discussions

An optical image of self-seeded AlN crystals after 10 h growth at 2080°C and 910 Torr is shown in Fig. 2. These needle and plate-like crystals were colorless and transparent. The growth rate was approximately 300 μm h^{-1} in the c-direction.

3.1. Photoluminescence

PL spectra for the AlN crystals along with the spectra from AlN crystals produced in a tungsten crucible and a BN crucible (for comparison) are shown in Fig. 3. Sample A was a polycrystalline AlN crystal grown in a resistively heated tungsten furnace employing self-seeding mechanism; sample B (single crystal) was produced in a BN crucible in the microwave furnace described above; sample C (single crystal) was grown in pBN crucibles using graphite heating-element reactor; and sample D was original sintered AlN (raw source materials). All samples other than sample D were nominally pure AlN crystals, except for residual impurities from the source and impurities introduced from the growth ambient. According to Refs. [15,16],
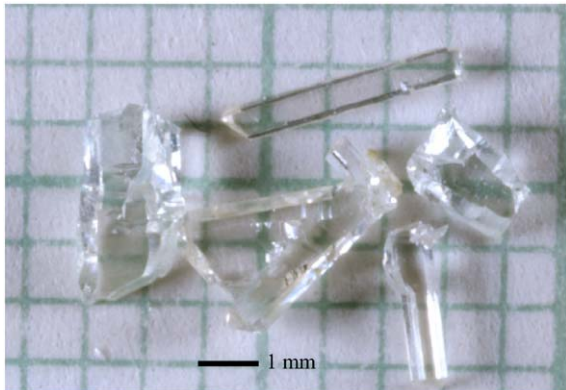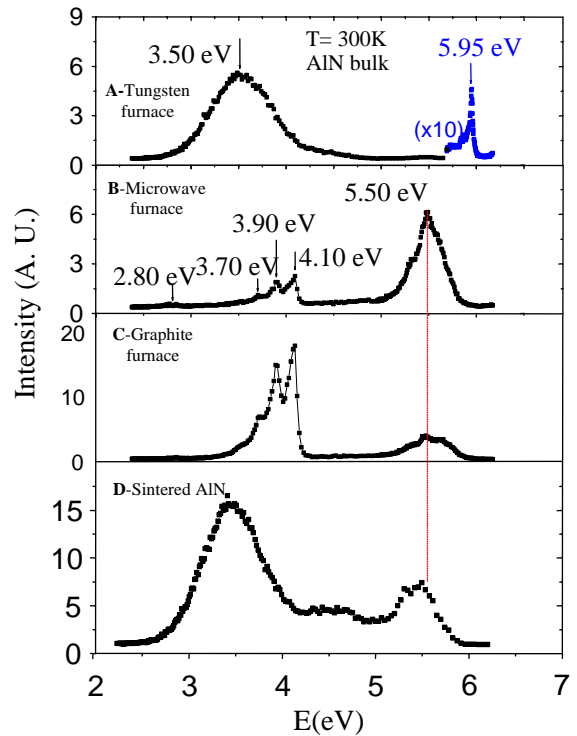

Fig. 3. PL spectra of AlN crystals produced in tungsten furnace (A), microwave furnace (B), graphite furnace (C) and raw source materials (D).

sample A has a near-band-edge emission of 5.95 eV (at room temperature), which is believed to be due to free excitons or excitons bond to shallow impurities (presumably tungsten). This near-band-edge emission disappeared in PL of samples B and C. Instead PL peaks at 5.50 eV are clearly visible. This might indicate the presence of Mg impurities in the AlN following the result of Nam et al. [17] on Mg-doped AlN. In agreement with this conclusion composition analysis using laser ablation mass spectrometry finds the presence of a Mg in the crystals. Its results are shown in Table 1. Meanwhile, considering the fact that the PL spectrum of raw source materials (spectrum D in Fig. 3) also has a peak at 5.50 eV, we believe Mg impurity presumably comes from the source materials, from which the crystals were grown. Further work is needed to obtain better understanding of the origins of the peaks at 4.10, 3.90, 3.70 and 2.80 eV.

Fig. 2. Self-seeded AlN crystals after 10 h growth at 2080°C and 910 Torr.

3.2. Raman analysis

Generally in Raman spectra of AlN, the width (FWHM) of the E_2 (high) Raman peak reflects the material's crystalline quality, and the E_2 (high) phonon frequency is sensitive to stress [18]. Fig. 4 shows the Raman spectrum from an AlN crystal produced in the microwave furnace. Strongly visible are the symmetry-allowed E_2 (high) and A_1 (TO) Raman modes in the used $x(yy) - x$ scattering geometry. The E_2 (high) peak position is $656.0\,cm^{-1}$ and the FWHM is $6.6\,cm^{-1}$. This

Table 1
Compositional analysis (ppm)

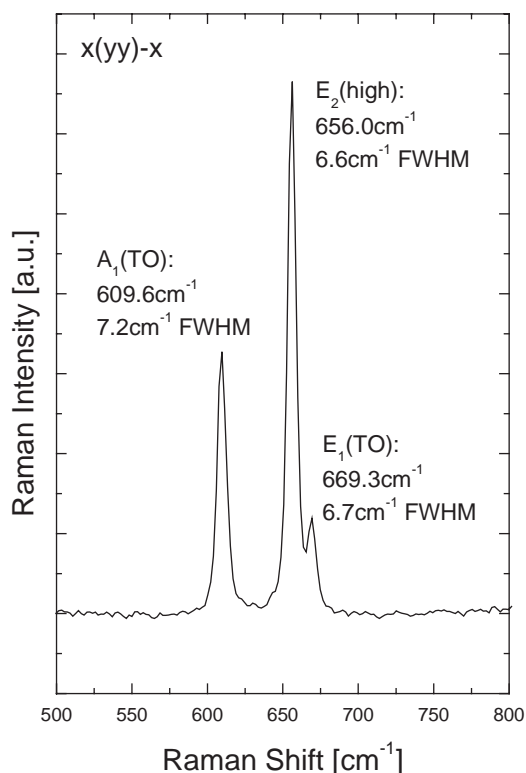| Sample	Crucible	Carbon	Magnesium	Silicon	Iron
B	BN	10,920	2772	2003	521
C	pBN	6561	2985	1968	858

Fig. 4. Raman spectrum of AlN crystal produced in microwave furnace, recorded in $x(yy)$-x scattering geometry.

FWHM value is slightly improved with respect to other bulk AlN crystals reported in the literature [19], i.e., indicating improvements in crystalline quality with the new technique. The E_2 (high) phonon frequency is similar to values reported for stress-free AlN [20,21].

3.3. Eutectic etch and SWBXT

Etching of AlN in molten eutectic potassium hydroxide (59 wt%) and sodium hydroxide (41 wt%) is an effective method for studying dislocation types, densities, and distributions, just as it is for GaN [22–24]. The shape of etching features formed in these studies is similarly dependent on the crystal polarity due to AlN's identical structure and chemical bonding with GaN (wurtzite).

Since AlN heteroepitaxial film always has Al-polar when growing on Si face SiC substrate [25], the etching condition for such sample was used to determine etching parameters of Al-polar microwave generated crystals. The optimized etching condition for heteroepitaxial AlN [26] is 2 min at $350°C$ in eutectic KOH/NaOH. It is expected that the microwave generated AlN crystal has a better quality than heteroepitaxial crystals, thus we etched such crystals at slight higher temperature ($380°C$) and for longer time (3 min). The results were shown in Fig. 5. The calculated defect density is $6.06 \times 10^3\,cm^{-2}$. The SWBXT pattern (defect density = $5.99 \times 10^3\,cm^{-2}$ shown in Fig. 6) of AlN crystal from the same run, confirmed that defect density of microwave generated AlN crystal on Al-polar is on the order of magnitude of $6 \times 10^3\,cm^{-2}$, which was immensely reduced compared to bulk AlN seeded grown on 6H–SiC substrate ($10^7\,cm^{-2}$) [26,27]. Details of eutectic etching of AlN crystals will be reported elsewhere [27].

4. Concluding remarks and expectation

A new technique for bulk AlN single crystal growth employing microwaves as the heat source was successfully demonstrated. The crystals have good structural quality, as indicated by Raman spectra, etch pit density and SWBXT studies. It is
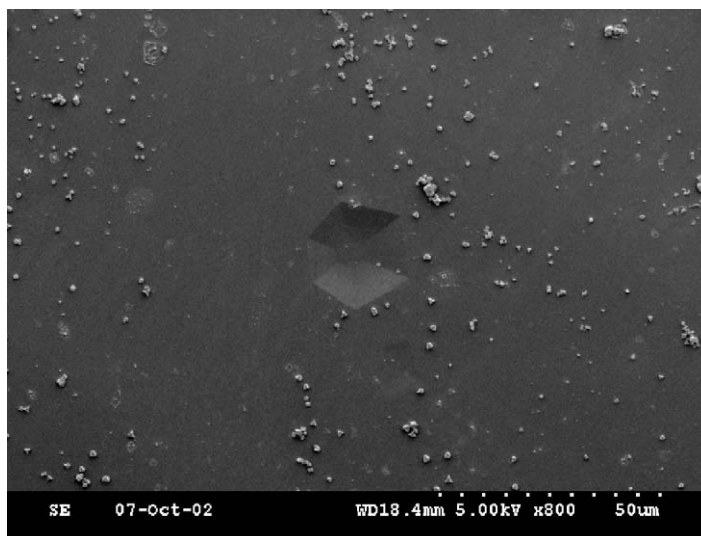
Fig. 5. SEM image of Al-polar AlN crystal produced in microwave furnace after 3 min etch at 380°C in eutectic KOH/NaOH alloy.
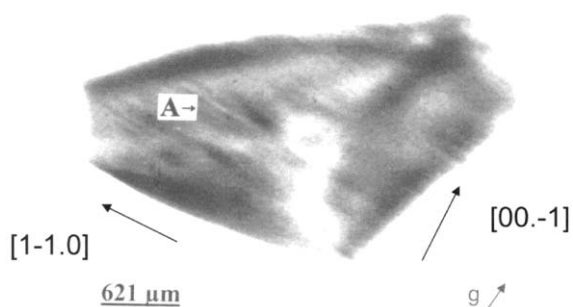

Fig. 6. SWBXT in transmission from the sample # 04-08-02, A = dislocation slip line, $g = 038$ reflection, wavelength $\lambda = 0.05049$ nm. Dislocation density $= 5.99 \times 10^3$ cm^{-2}.

believed that this technique is advanced in preventing damages of the furnace fixtures since the source materials can be heated to elevated temperature ($> 2000°C$), while the crucible temperature is kept in a relatively low range. The future work will focus on scaling up crystal size and seeded growth for effective control of crystalline orientation.

Acknowledgements

References

[1] T. Mukai, S. Nagahama, N. Iwasa, N. Senoh, T. Yamada, J. Phys. Condes. Matter 13 (2001) 7089.
[2] O. Ambacher, J. Phys. D 31 (1998) 2653.
[3] J.H. Edgar (Ed.), Properties of Group III Nitrides, Electronic Materials Information Service (EMIS), London, 1994.
[4] M. Kuball, J.M. Hayes, M.J. Uren, T. Martin, J.C.H. Birbeck, R.S. Balmer, B.T. Hughes, IEEE Electron Dev. Lett. 23 (2002) 7.
[5] G.A. Slack, T.F. McNelly, J. Crystal Growth 34 (1976) 263.
[6] L. Liu, J.H. Edgar, J. Crystal Growth 220 (2000) 243.
[7] J.D. Katz, Annu. Rev. Mater. Sci. 22 (1992) 152.
[8] R.W. Francis, W.L. Worrell, J. Electrochem. Soc. 123 (1976) 430.
[9] H.E. Huey, Q.S. Wang, et al., Ceram. Eng. Sci. Proc. 21 (4) (2000) 599.
[10] J.H. Harris, R.A. Youngman, R.G. Teller, J. Mater. Res. 5 (1990) 1763.
[11] L.E. McNeil, M. Grimsditch, R.H. French, J. Am. Ceram. Soc. 76 (1993) 1132.

[12] E. Kuokstis, J. Zhang, Q. Fareed, J.W. Yang, G. Simin, M.A. Khan, R. Gaska, M. Shur, C. Rojo, L. Schowalter, Appl. Phys. Lett. 81 (15) (2002) 2755.

[13] G.A. Slack, R.A. Tanzilli, R.O. Pohl, J.W. Vandersande, J. Phys. Chem. Solids 48 (1987) 641.

[14] X. Tang, F. Hossain, K. Wongchotigul, M.G. Spencer, Appl. Phys. Lett. 72 (12) (1998) 1501.

[15] J. Li, K.B. Nam, M.L. Nakarmi, J.Y. Lin, H.X. Jiang, Appl. Phys. Lett. 81 (18) (2002) 3365.

[16] K.B. Nam, J. Li, M.L. Nakarmi, J.Y. Lin, H.X. Jiang, Appl. Phys. Lett. 82 (11) (2002) 1694.

[17] K.B. Nam, M.L. Nakarmi, J.Y. Lin, H.X. Jiang, Appl. Phys. Lett. 83 (5) (2002) 878.

[18] M. Kuball, Surf. Interface Anal. 31 (2001) 987.

[19] M. Kuball, J.M. Hayes, Y. Shi, J.H. Edgar, Appl. Phys. Lett. 77 (2000) 1958.

[20] J.M. Hayes, M. Kuball, Y. Shi, J.H. Edgar, Jpn. J. Appl. Phys. 39 (2000) L710.

[21] V.Y. Davydov, Y.E. Kitaev, I.N. Goncharuk, A.N. Smirnov, J. Graul, O. Semchinova, D. Uffmann, M.B. Smirnov, A.P. Mirgorodsky, R.A. Evarestov, Phys. Rev. B 58 (1998) 12899.

[22] J.L. Weyher, P.D. Brown, J.L. Rouviere, T. Wosinski, A.R.A. Zauner, I. Grzegory, J. Crystal Growth 210 (2000) 151.

[23] G. Kamler, J.L. Weyher, I. Grzegory, E. Jezierska, T. Wosinski, J. Crystal Growth 246 (2002) 21.

[24] J.L. Weyher, L. Macht, G. Kamler, J. Borysiuk, I. Grzegory, Phys. Stat. Sol. c 0 (3) (2003) 821.

[25] D. Zhuang, J.H. Edgar, L. Liu, B. Liu, L. Walker, MRS Int. J. Nitride Semicond. Res. 7 (2002) 4.

[26] Y. Shi, B. Liu, L. Liu, J.H. Edgar, E.A. Payzant, J.M. Hayes, M. Kuball, MRS Internet J. Nitride Semicond. Res. 6 (2001) 5.

[27] D. Zhuang, J.H. Edgar, B. Strojek, J. Chaudhuri, Z. Rek, J. Crystal Growth 262 (2004) 89.